Stress Response Optimization of Elastic/Viscoelastic Composite Strips

Rich Laverty, Davies Fellow
US Army Research Laboratory and
Department of Mathematical Sciences
United States Military Academy
West Point, New York 10996

George Gazonas, Research Physicist
US Army Research Laboratory
Weapons and Materials Research Directorate
Aberdeen Proving Ground, Maryland 21005

1 Executive Summary

We consider four boundary value problems (BVPs), concerning ourselves with the transient response of elastic/viscoelastic strips subject to different boundary conditions (BCs). Although each problem is of a fundamental interest in basic mechanics, the primary purpose for these models is to find situations where the composite strips admit optimal designs. The models that do possess optimal designs can then be used as benchmarks for larger, numerical studies of more complicated materials and geometries.

Of the four problems considered, only the strip subject to a stress step and fixed at the far end has optimal solutions. The qualitative structure of these solutions mimics those of the elastic/elastic strip considered in the introduction. Despite the lack of optimal solutions for the other cases we do see that the impact boundary conditions differ significantly from the stress step conditions in that the peak stress decreases with distance from the applied stress. This is in sharp contrast with the motivating BVP presented in the introduction where the peak stress is greater at greater distances from the applied stress.

In all the problems considered the method of solution is the Laplace transform with a numerical inversion via the DAC algorithm. Details and further references for this method can be found in the appendix.

2 Introduction

For background and motivation, we consider a special case of a problem from Velo and Gazonas, [1]. A description of the physical situation is this: A strip composed of two elastic layers is subject to a step in stress on one boundary and the other boundary is kept fixed. Mathematically, the BVP presented in Table 1 summarizes the situation:

Table 1. The BVP corresponding to two elastic layers subject to a step stress on the left and fixed on the right.

	Layer 1, $0 < x < L/2$	Interface, $x = L/2$	Layer 2, $L/2 < x < L$
PDEs	$\frac{\partial^2 u_1}{\partial t^2} = c_1^2 \frac{\partial^2 u_1}{\partial x^2}$		$\frac{\partial^2 u_2}{\partial t^2} = c_2^2 \frac{\partial^2 u_2}{\partial x^2}$
ICs	$u_1(x,0) = 0$ $\frac{\partial u_1}{\partial t}(x,0) = 0$		$u_2(x,0) = 0$ $\frac{\partial u_2}{\partial t}(x,0) = 0$
BCs	$\sigma_0 H(t) = E_1 \frac{\partial u_1}{\partial x}(0,t)$	$u_1\left(\frac{L}{2},t\right) = u_2\left(\frac{L}{2},t\right)$ $E_1 \frac{\partial u_1}{\partial x}\left(\frac{L}{2},t\right) = E_2 \frac{\partial u_2}{\partial x}\left(\frac{L}{2},t\right)$	$u_2(L,t) = 0$

We will further limit the possible selection of materials for Layer 2 by introducing the parameter α and using it to scale both the elastic modulus and density of Layer 1:

$$E_2 = E_1 / \alpha$$
$$\rho_2 = \rho_1 / \alpha$$

This restriction implies that waves propagating in each layer will propagate with the same velocity, i.e.,

$$c_1 = c_2 .$$

Pretending there exists a strain gauge at the center of each layer, we would record stress/time histories that are displayed in Figure 1.

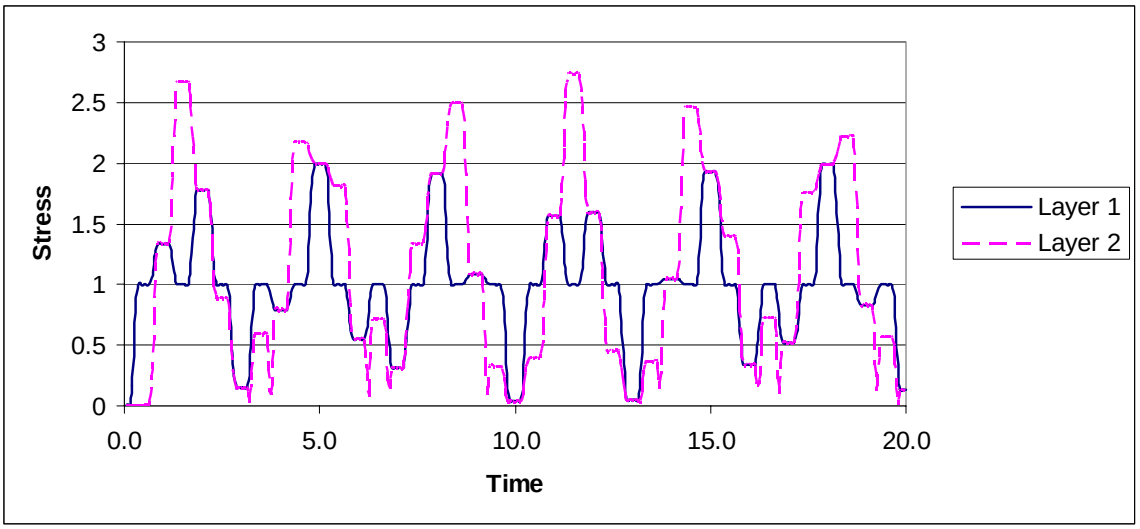

Figure 1. The stress/time history at the center of each layer of an elastic/elastic strip with a parameter value $\alpha = 0.5$. Stress is normalized by the magnitude of the applied stress, σ_0, and time is normalized by the propagation time across the entire composite, L/c.

A feature of Figure 1 that leads to further inquiry is that the stress in Layer 2 seems to exceed that of Layer 1 by a considerable amount. Is this true for every value of α? Figure 2 is a graph of the peak stresses that propagate in Layers 1 and 2 as α is varied from 0 to 10.

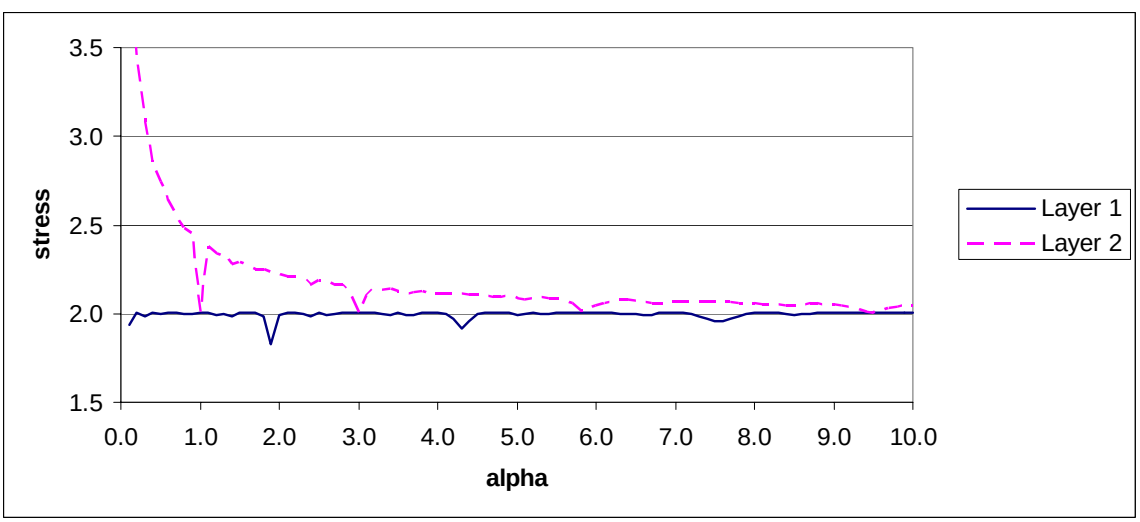

Figure 2. The peak stress in each layer as a function of α.

There appear to be, in Figure 2, values of α for which the peak stress in Layer 2 is at a minimum, and this minimum value appears to be 2. This is in fact the case and one of the results reported in [1]. To summarize the relevant facts from that paper, the peak stress in Layer 1 is always less than or equal to 2, the peak stress in Layer 2 is always greater than or equal 2 and there are an infinite number of values of α for which the limiting values of peak stress will be achieved. We will refer to these values of α as "optimal designs."

The existence of optimal designs is the starting point and motivation for the current study. The existence, however, is not always guaranteed. For instance, consider the same strip with the fixed boundary at the right replaced by a free boundary:

$$E_2 \frac{\partial u_2}{\partial x}(L,t) = 0 .$$

Now, if we vary α and record the corresponding peak stresses in Layer 1 and 2 we get Figure 3.

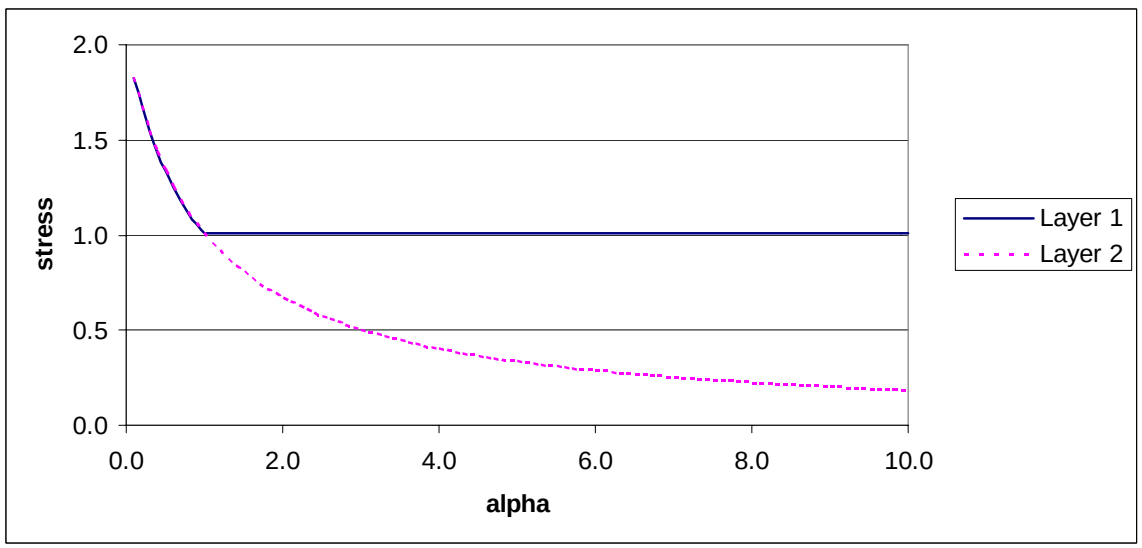

Figure 3. The peak stresses propagated in an elastic/elastic strip subject to a stress step on one boundary and free on the other.

Given such unexpected behavior in such simple models, we wish to answer the following questions: Can a slight change of materials still lead to a situation with optimal designs? Can a slight change in the applied stress lead to optimal designs? We answer these questions in the sections that follow using a standard linear viscoelastic material in Layer 2. We will consider separately the cases where the stress is generated by a stress step and a low velocity impact by a massive rigid solid. We will also vary the condition on the right between a fixed and free boundary.

3 Elastic/Viscoelastic strip subject to a stress step

We will start by formulating the appropriate BVP for a strip composed of an elastic layer, subject to a step in stress, perfectly bonded to a viscoelastic layer fixed at its far end.

Table 2. BVP for the elastic/viscoelastic strip subject to a stress step on the left and fixed on the right.

	Layer 1, $0 < x < L/2$	Interface, $x = L/2$	Layer 2, $L/2 < x < L$
PDEs	$\frac{\partial^2 u_1}{\partial t^2} = c_1^2 \frac{\partial^2 u_1}{\partial x^2}$		$\frac{\partial^2 u_2}{\partial t^2} = \frac{1}{\rho_2}\frac{\partial}{\partial x}\left(G * \frac{\partial \varepsilon_2}{\partial t}\right)$
ICs	$u_1(x,0) = 0$ $\frac{\partial u_1}{\partial t}(x,0) = 0$		$u_2(x,0) = 0$ $\frac{\partial u_2}{\partial t}(x,0) = 0$
BCs	$\sigma_0 H(t) = E_1 \frac{\partial u_1}{\partial x}(0,t)$	$u_1\left(\frac{L}{2},t\right) = u_2\left(\frac{L}{2},t\right)$ $E_1 \frac{\partial u_1}{\partial x}\left(\frac{L}{2},t\right) = \left[G * \frac{\partial \varepsilon_2}{\partial t}\right]_{x=\frac{L}{2}}$	$u_2(L,t) = 0$

We have employed the following notations: The strain is denoted by ε and $*$ denotes a convolution. Therefore, the strain-displacement relation for Layer 2 is

$$\varepsilon_2 = \frac{\partial u_2}{\partial x}.$$

There are many equivalent ways to prescribe viscoelastic behavior and we have chosen to use the relaxation modulus, $G(t)$. This function gives the stress response of the solid to an experiment where a unit strain is applied and held. The resulting stress, $G(t)$, is a decaying function of time. Thus, the stress in Layer 2, is expressed as a convolution, in time, of the relaxation modulus and the time derivative of the strain, [2,3],

$$\begin{aligned}\sigma_2(x,t) &= G(t) * \frac{\partial \varepsilon_2}{\partial t}(x,t) \\ &= \int_0^t G(t-\tau)\frac{\partial \varepsilon_2}{\partial \tau}(x,\tau)\,d\tau\end{aligned}$$

We will be considering the case where Layer 2 is a standard linear solid. Its relaxation behavior is characterized by an initial elastic response, G_0, followed by exponential decay towards a long time stress G_∞.

$$G(t) = G_\infty + (G_\infty - G_0)e^{-\beta t}$$

To keep the situation analogous to that considered in the introduction, we will scale the density and the initial elastic response by the parameter α. This will also keep the wavefronts moving with the same velocity in both layers.

$$G_0 = E_1 / \alpha$$
$$\rho_2 = \rho_1 / \alpha$$

If we record the peak stresses in each layer as α is varied we would get the graphs in Figure 4.

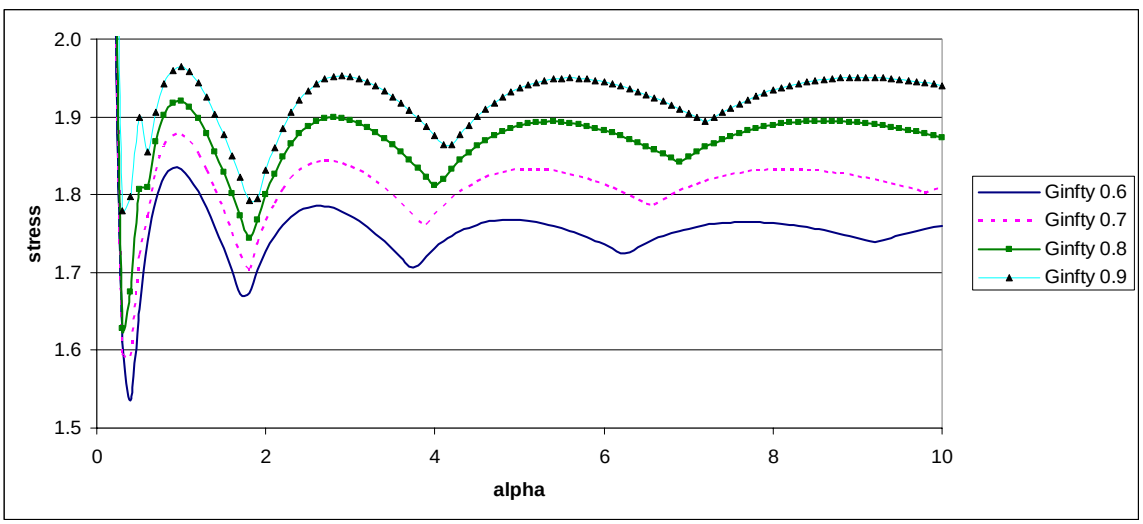

Figure 4. The peak stress propagated in Layer 2 (visco layer) for several values of G_∞ (relative to G_0) as α is varied. In each case the decay parameter is $\beta = 1$.

So, we have struck upon another situation where optimal designs exist. From Figure 4 we can see a slight sensitivity of the optimal designs to the long term behavior of the viscoelastic solid, G_∞, but the qualitative behavior is consistent throughout all values considered.

We can also look at the peak stress in the elastic layer and see similar results, Figure 5.

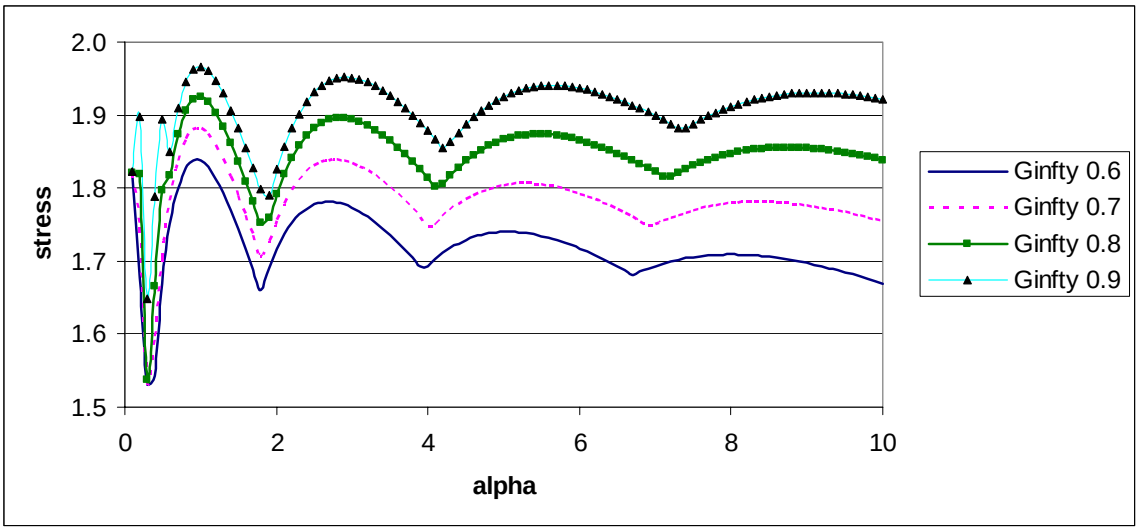

Figure 5. The peak stress in Layer 1, the elastic layer.

In Figure 5 we see one interesting behavior that was not present in the elastic/elastic case. The optimal designs for the layers almost correspond; whereas, in the elastic/elastic case, the minimum of peak stress in Layer 2 occurred at parameter values where the peak stress in Layer 1 was at a maximum. Consider Figure 6:

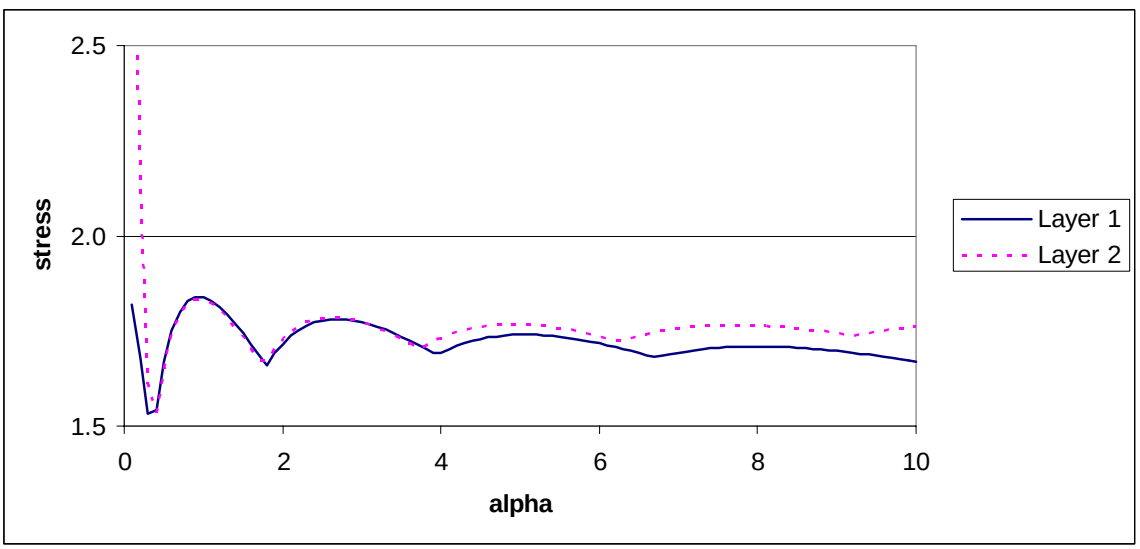

Figure 6. The peak stresses in each layer of an elastic/viscoelastic strip with $G_\infty = 0.6G_0$.

For low values of α the peak stresses almost coincide. Therefore, an optimal design would be near optimal for both layers, not just Layer 2.

Now consider the case where Layer 2 is free instead of fixed at $x = L$.

$$\left[G * \frac{\partial \varepsilon_2}{\partial t} \right]_{x=L} = 0$$

This is analogous to the case illustrated in Figure 3 of the previous section. And, as in that section we can see, Figure 7, that this situation has lead to no optimal designs. In fact, there appears to be little advantage to using the viscoelastic layer vice the purely elastic layer when the back boundary of the strip is free.

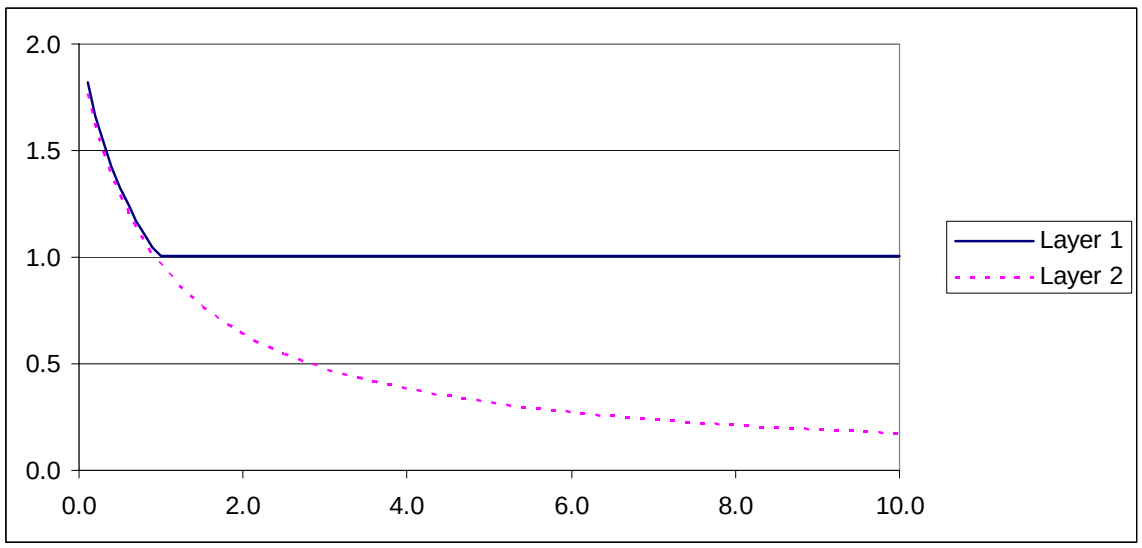

Figure 7. The peak stresses in the elastic/viscoelastic strip when the right end of the composite is left free. Material parameters used in this model were $G_\infty = 0.7G_0$ and $\beta = 1$.

4 The Elastic/Viscoelastic strip subject to a rigid impact

We want to use the same strip that we used in the previous section, but now we will generate stress waves via low-velocity impact by a rigid projectile. The following table is a formulation of the appropriate BVP:

Table 3. Formulation of the BVP for rigid impact upon a fixed elastic/viscoelastic strip.

	Striker	Interface 1, $x=0$	Layer 1, $0<x<L/2$	Interface 2, $x=L/2$	Layer 2, $L/2<x<L$
PDEs	$m\frac{d^2u_0}{dt^2}=E_1\frac{\partial u_1}{\partial x}$		$\frac{\partial^2 u_1}{\partial t^2}=c_1^2\frac{\partial^2 u_1}{\partial x^2}$		$\frac{\partial^2 u_2}{\partial t^2}=\frac{1}{\rho_2}\frac{\partial}{\partial x}\left(G*\frac{\partial \varepsilon_2}{\partial t}\right)$
ICs	$u_0(0)=0$ $\frac{du_0}{dt}(0)=v_0$		$u_1(x,0)=0$ $\frac{\partial u_1}{\partial t}(x,0)=0$		$u_2(x,0)=0$ $\frac{\partial u_2}{\partial t}(x,0)=0$
BCs		$u_0(t)=u_1(0,t)$		$u_1\left(\frac{L}{2},t\right)=u_2\left(\frac{L}{2},t\right)$ $E_1\frac{\partial u_1}{\partial x}\left(\frac{L}{2},t\right)=\left[G*\frac{\partial \varepsilon_2}{\partial t}\right]_{x=\frac{L}{2}}$	$u_2(L,t)=0$

It should be pointed out that this BVP is only valid until contact between the striker and the strip is lost. From that point on, the strip will undergo free vibrations. For the results that follow, we have only considered the stresses that propagate while this BVP is valid. Therefore, if, under free vibrations, the strip would have attained a greater peak stress then that will not be reflected in our results.

Figure 8 is a graph of the peak stress as a function of the parameter α, which plays the same role as in the previous section.

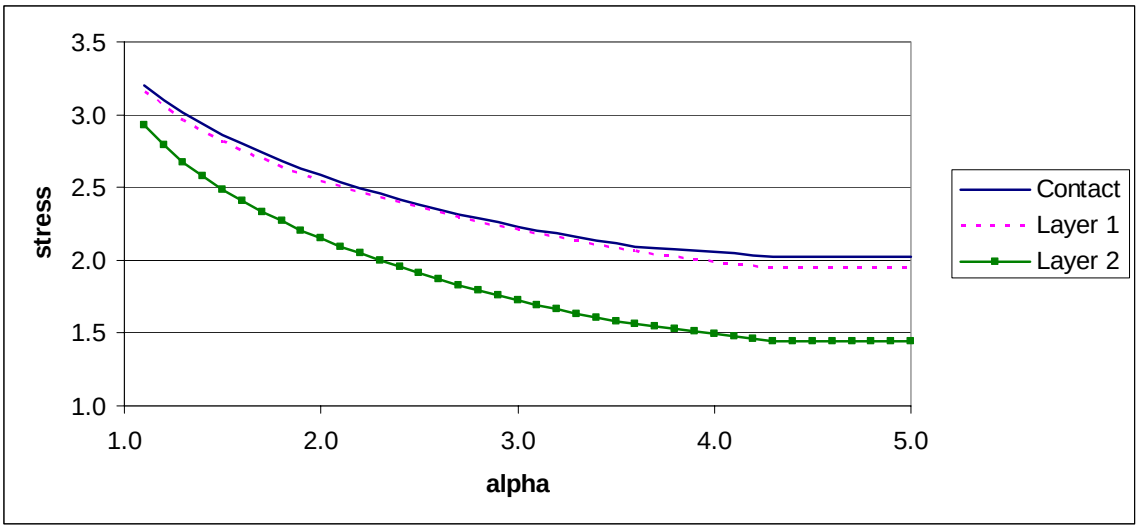

Figure 8. The peak stress at the point of contact and at the center of each layer as a function of α. The viscoelastic material parameters are $G_\infty = 0.7G_0$ and $\beta = 10$. The striker has a mass of 12 times the composite strip and the normalizing stress is now $\sigma_0 = v_0\sqrt{E_1\rho_1}$.

Again, we are left without any optimal designs. One difference between the stress step and the impact scenarios is that during impact, the peak stress decreases monotonically with distance from the point of impact. This is in sharp contrast to the elastic/elastic strip subject to a stress step where the peak stress in Layer 2 was always greater than the peak stress in Layer 1.

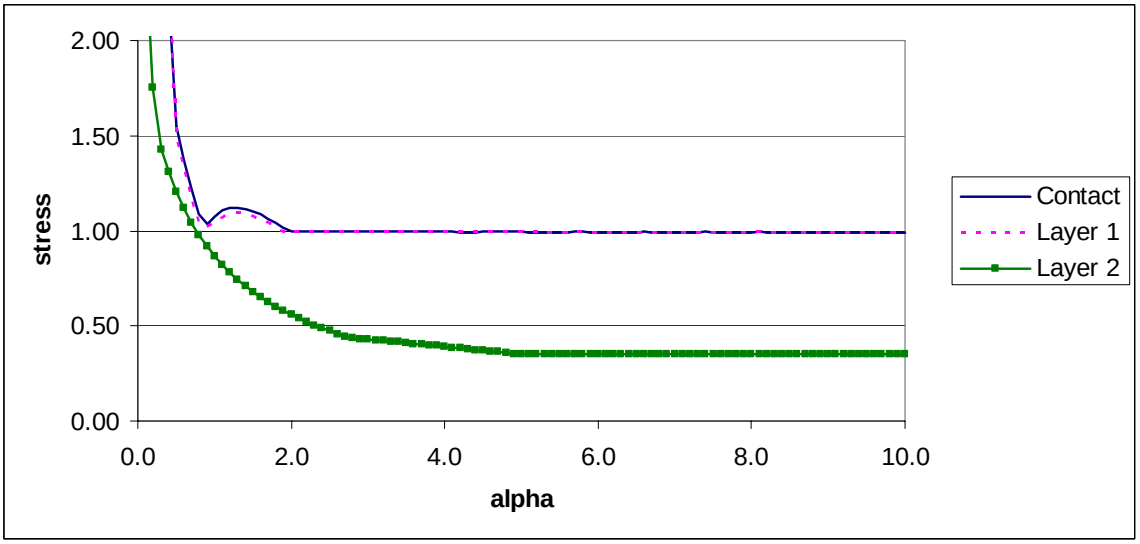

Figure 9. The peak stresses at the point of contact and the midpoint of Layer 1 and 2. Stress is generated by impact by a rigid projectile of relative mass of 12. The strip is free on the far end.

Figure 9 gives the results for the last case considered here. This is the rigid impact where the strip is free on the far boundary. Clearly, for Layer 2 there are no optimal designs, and for most of the values of α shown, the peak stress in Layer 1, at the point of contact and the midpoint of the layer, follows a similar path. There is some interesting behavior when $1 < \alpha < 2$, but we don't see the type of behavior we seek. If we take the relative stress of 1 to be the minimum of the peak stress (in Layer 1), then any value of α greater than 2 will provide this value.

Layer 2 approaches its large α behavior more smoothly, but there are still no local minimums.

7 Summary

We have considered four simple BVPs. In each, an elastic/viscoelastic strip is subject to varying BCs and one parameter is allowed to vary. As that parameter varies we seek optimal designs with respect to the peak stress.

In the case of a stress step applied to a fixed strip, the optimal designs follow a qualitatively similar pattern to the elastic/elastic strip. None of the other cases display this behavior. Both the stress step/free and the rigid impact/fixed BVPs have a monotonically decreasing peak stress for all values of the parameter in each layer. The rigid impact/free BVP has a limited range of parameter values where peak stress does not follow this monotonic behavior, but it is very limited and the single minimum value of peak stress is not found at distinct parameter values.

Acknowledgements

This work was performed while the first author held a National Research Council Research Associateship Award at the Army Research Laboratory and the United States Military Academy.

References

[1] Velo, Ani P. and Gazonas, George A., "Optimal design of a two-layered elastic strip subjected to a transient loading," *Int'l J. Solids and Structures*, Vol. 40, 2003, pp. 6417-6428.

[2] Flugge, Wilhelm, *Viscoelasticity, 2nd Revised Edition*, Springer-Verlag, Berlin, 1975.

[3] Christensen, Richard M., *Theory of Viscoelasticity, 2nd Edition*, Dover Publications, Inc., Mineola, NY, 2003.

[4] Laverty, Richard R. and Gazonas, George A., "Laplace Transform Inversion and Viscoelastic Wave Propagation," *Proceedings of the 11th Annual ARL/USMA Technical Symposium*, 2003, pp. 1-23.

[5] Dubner H. and Abate J., "Numerical Inversion of Laplace Transforms by Relating Them to the Finite Fourier Cosine Transform," *J. Assoc. for Comp. Mach*., Vol. 15, No. 1, 1968, pp. 115-123.

[6] Crump, Kenny S., "Numerical Inversion of Laplace Transforms Using a Fourier Series Approximation," *J. Assoc. for Comp. Mach*., Vol. 23, No. 1, 1976, pp. 89-96.

[7] Durbin, F., "Numerical inversion of Laplace transforms: an efficient improvement to Dubner and Abate's method," *Comp. J*., Vol. 17, No. 4, 1974, pp. 371-376.

[8] LePage, Wilbur R., *Complex Variables and the Laplace Transform for Engineers*, Dover Publications, Inc., New York, NY, 1980.

[9] Lanczos, Cornelius, *Discourse on Fourier Series*, Hafner Publishing Company, New York, 1966.

Appendix: Computational Method

In transient problems it is often convenient to use the Laplace transform as a method for solving differential equations. In the case of viscoelastic materials, due to the Correspondence Principle, Laplace transforms *are* the essential tool. Therefore, in this study Laplace transforms have been used for all calculations. However, because of the variety and complexity of transforms encountered it was decided that numerical inversion would provide the most efficient means towards a solution in the time domain.

In a related study by the same authors, [4], it was concluded that the most appropriate method for numerical inversion was the DAC algorithm, [5,6,7]. It is the purpose of this appendix to briefly describe the algorithm and its modification for handling the Gibbs' phenomenon present in all of the problems considered.

Consider a Laplace transform pair, defined by the integrals:

$$\hat{f}(s) = \int_0^\infty f(t) e^{-st} dt$$

$$f(t) = \frac{1}{2\pi i} \int_{a-i\infty}^{a+i\infty} \hat{f}(s) e^{st} ds$$

The real number a in the inversion integral is taken to be greater than the real part of any singularities of the transform $\hat{f}(s)$. For details about the classes of permissible functions and issues of convergence we refer to any standard text, such as LePage, [8].

Since the inversion integral is taken along a vertical path in the s-plane, we fix the real part of s and set the variable of integration to the real variable ω, where $s = a + i\omega$. Then set $\hat{f} = u + iv$, where u and v are real valued. Expanding, and using the knowledge that $f(t)$ is real:

$$f(t) = \frac{e^{at}}{2\pi} \int_{-\infty}^{\infty} [u\cos(\omega t) - v\sin(\omega t)] d\omega$$

The products $u\cos(\omega t)$ and $v\sin(\omega t)$ are both even functions of ω; therefore, one further simplification yields the inversion formula:

$$f(t) = \frac{e^{at}}{\pi} \int_0^{\infty} [u\cos(\omega t) - v\sin(\omega t)] d\omega$$

If we approximate this integral using Simpson's rule with a step size of $\Delta\omega = \pi / T$, we get the series

$$f(t) \approx \frac{e^{at}}{T}\left[\frac{\hat{f}(a)}{2} + \sum_{k=1}^{\infty} u\left(a + \frac{k\pi i}{T}\right)\cos\left(\frac{k\pi t}{T}\right) - v\left(a + \frac{k\pi i}{T}\right)\sin\left(\frac{k\pi t}{T}\right)\right].$$

This series, once truncated, is the DAC approximation to the inversion integral. Error is introduced into the approximation through truncation of the series and because the Simpson's method was used to approximate the integral. These errors can be bounded by an appropriate choice of the real number a. A detailed analysis of error can be found in the references, [5,6,7].

One matter that concerns us is that the approximation is in the form of a Fourier series. Therefore, it is susceptible to Gibbs' phenomenon at discontinuities. This has lead to some poor quantitative results when optimizing the types of problems considered in this paper. For instance, in the very first problem considered, and elastic/elastic strip subject to a step in stress and fixed at the far end. Without mitigating for Gibbs', the peak stress in each Layer as a function of α can be seen in Figure 10.

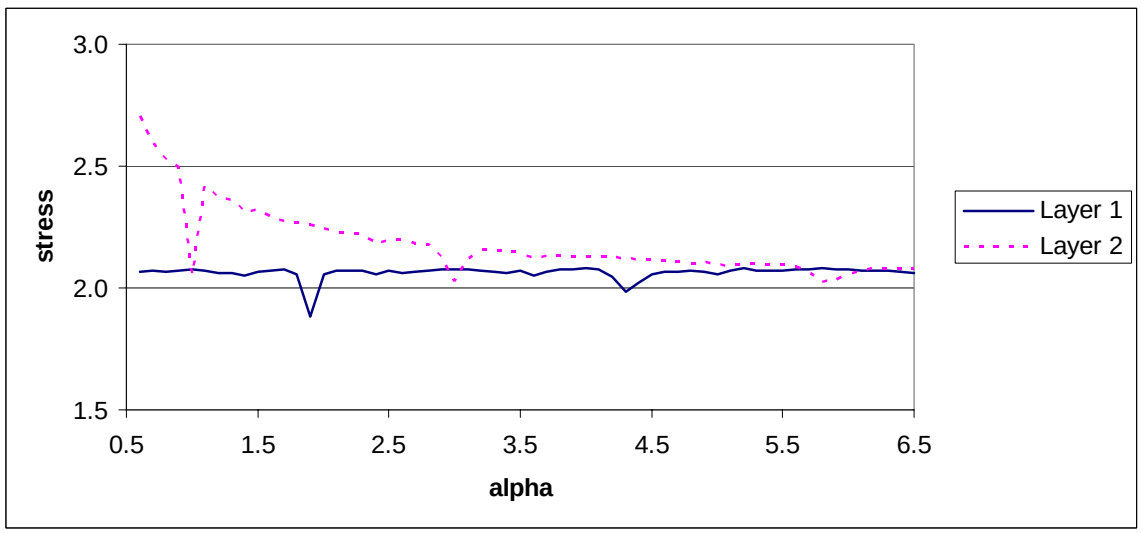

Figure 10. Optimization of an elastic/elastic strip, subject to a stress step and fixed at the far end. Results without mitigation of Gibbs' phenomenon.

We know, analytically [1], that the Layer 1 stress is always below 2 and the minimums of the Layer 2 stress should reach down to 2, but Figure 10 does not support this. This is the result of Gibbs' phenomenon, where the value of stress is overestimated at every wavefront.

To mitigate the effect of Gibbs' phenomenon we have employed a filter technique known as Lanczos' σ-factors, [9]. When a Fourier series is truncated at $k = N$, then the σ-factors are given by

$$\sigma_k = \frac{\sin\left(\frac{k\pi}{N}\right)}{\frac{k\pi}{N}}.$$

Thus, a truncated Fourier series for a function $g(t)$ on the interval $(0,2T)$ with Fourier coefficients a_k and b_k will take the form

$$g(t) \approx \frac{a_0}{2} + \sum_{k=1}^{N}\left[\sigma_k a_k \cos\left(\frac{k\pi t}{T}\right) + \sigma_k b_k \sin\left(\frac{k\pi t}{T}\right)\right].$$

The presence of the σ-factors does not effect the convergence of the series, introduces a minimum of computations into the DAC algorithm and works well at eliminating the effects of Gibbs' phenomenon.